THE JOURNAL OF BIOLOGICAL CHEMISTRY VOL. 281, NO. 43, pp. 32540–32549, October 27, 2006

Homer 1 Mediates Store- and Inositol 1,4,5-Trisphosphate Receptor-dependent Translocation and Retrieval of TRPC3 to the Plasma Membrane*

Received for publication, March 16, 2006, and in revised form, July 6, 2006 Published, JBC Papers in Press, August 3, 2006, DOI 10.1074/jbc.M602496200

Joo Young Kim[‡§], Weizong Zeng[‡], Kirill Kiselyov[¶], Joseph P. Yuan[‖], Marlin H. Dehoff[‖], Katsuhiko Mikoshiba[**], Paul F. Worley[‖1], and Shmuel Muallem[‡2]

*From the [‡]Department of Physiology, University of Texas Southwestern Medical Center, Dallas, Texas 75390, the [§]Department of Pharmacology, Institute of Gastroenterology, and Brain Korea 21 Project for Medical Science, Yonsei University College of Medicine, Seoul 120-752, Korea, the [¶]Department of Biological Sciences, University of Pittsburgh, Pittsburgh, Pennsylvania 15260, the [‖]Department of Neuroscience, Johns Hopkins University School of Medicine, Baltimore, Maryland 21205, and the **Department of Molecular Neurobiology, Institute of Medical Science, University of Tokyo, 4-6-1 Shirokanedai, Minato-ku, Tokyo 108-8639, Japan*

Store-operated Ca^{2+} channels (SOCs) mediate receptor-stimulated Ca^{2+} influx. Accumulating evidence indicates that members of the transient receptor potential (TRP) channel family are components of SOCs in mammalian cells. Agonist stimulation activates SOCs and TRP channels directly and by inducing translocation of channels in intracellular vesicles to the plasma membrane (PM). The mechanism of TRP channel translocation in response to store depletion and agonist stimulation is not known. Here we use TRPC3 as a model to show that IP_3 and the scaffold Homer 1 (H1) regulate the rate of translocation and retrieval of TRPC3 from the PM. In resting cells, TRPC3 exists in TRPC3-H1b/c-IP_3Rs complexes that are located in part at the PM and in part in intracellular vesicles. Binding of IP_3 to the IP_3Rs dissociates the interaction between IP_3Rs and H1 but not between H1 and TRPC3 to form IP_3Rs-TRPC3-H1b/c. TIRFM and biotinylation assays show robust receptor- and store-dependent translocation of the TRPC3 to the PM and their retrieval upon termination of cell stimulation. The translocation requires depletion of stored Ca^{2+} and is prevented by inhibition of the IP_3Rs. In HEK293, dissociating the H1b/c-IP_3R complex with H1a results in TRPC3 translocation to the PM, where it is spontaneously active. The TRPC3-H1b/c-IP_3Rs complex is reconstituted by infusing H1c into these cells. Reconstitution is inhibited by IP_3. Deletion of H1 in mice markedly reduces the rates of translocation and retrieval of TRPC3. Conversely, infusion of H1c into $H1^{-/-}$ cells eliminates spontaneous channel activity and increases the rate of channel activation by agonist stimulation. The effects of H1c are inhibited by IP_3. These findings together with our earlier studies demonstrating gating of TRPC3 by IP_3Rs were used to develop a model in which assembly of the TRPC3-H1b/c-IP_3Rs complexes by H1b/c mediates both the translocation of TRPC3-containing vesicles to the PM and gating of TRPC3 by IP_3Rs.

Ca^{2+} influx is a critical component of the receptor-evoked Ca^{2+} signal and plays a role in many physiological functions (1). The best described form of Ca^{2+} influx is mediated by the store-operated Ca^{2+} channels (SOCs),[3] which are activated by agonist-dependent or agonist-independent depletion of Ca^{2+} stored in the ER (1). The molecular identity of the SOCs and I_{crac} is still not known with certainty, although recent work points to ORAI1/CRACM1/olf186-F as a potential I_{crac} (2–5). However, accumulating evidence indicates that members of the transient receptor potential (TRP) family of ion channels are associated with SOCs in mammalian cells. Thus, deletion of TRPC4 in mice (6, 7) or of TRPC1, TRPC3, TRPC6, and TRPC7 by antisense or siRNA (8–10) and dominant negative TRPC1, TRPC3, or TRPC5 (11–14) partially inhibit SOCs and/or receptor-stimulated Ca^{2+} influx.

The mechanism by which agonist stimulation activates Ca^{2+} influx by TRPC channels is not well understood. TRPC1, -4, and -5 can be activated by store depletion, whereas TRPC3, -6, and -7 can be activated by the lipid diacylglycerol (11, 15, 16). However, depending on cell type and expression levels, TRPC3 can also be activated by store depletion (17–19). Several mechanisms have been proposed to explain how store depletion leads to activation of SOCs and TRPC channels; conformational coupling between TRPC channels and IP_3 receptors (IP_3Rs) (18, 20–22), exocytotic insertion of the channels in the plasma membrane (PM) (23–25), and activation by a diffusible messenger (26, 27). Biochemical and functional evidence showed regulatory interaction between IP_3Rs and several TRPC channels, including TRPC1 and TRPC3 (18, 28–32). The interaction between TRPC1 and IP_3Rs and gating of TRPC1 by IP_3Rs is mediated by Homers (33). Homers are scaffolding proteins that bind many Ca^{2+}-signaling proteins, including all TRPC channels and IP_3Rs (33–37). In addition, a C-terminal domain

* This work was supported by National Institutes of Health Grants DK38938 and DE12309 and by a Postdoctoral Fellowship Program of the Korea Science and Engineering Foundation. The costs of publication of this article were defrayed in part by the payment of page charges. This article must therefore be hereby marked "*advertisement*" in accordance with 18 U.S.C. Section 1734 solely to indicate this fact.

[1] To whom correspondence may be addressed. E-mail: pworley@jhmi.edu.
[2] To whom correspondence may be addressed. E-mail: Shmuel.Muallem@UTSouthwestern.edu.

[3] The abbreviations used are: SOC, store-operated Ca^{2+} channel; TRP, transient receptor potential; TRPC, canonical transient receptor potential channel; IP_3, inositol 1,4,5-trisphosphate; IP_3R, inositol 1,4,5-trisphosphate receptor; I_{crac}, Ca^{2+} release-activated current; PM, plasma membrane; ER, endoplasmic reticulum; WT, wild type; TIRFM, total internal reflection microscopy; CPA, cyclopiasonic acid; IP, immunoprecipitation; PBS, phosphate-buffered saline; GST, glutathione *S*-transferase; YFP, yellow flourescent protein.

of several TRPC channels directly interacts with an N-terminal sequence in the IP_3Rs (28, 32) that participates in gating of TRPC channels by IP_3Rs (30, 32).

A newly discovered and apparently a general regulatory mechanism of TRPC channel activity is agonist-stimulated translocation of the channels to the PM. In HEK293 cells, receptor stimulation but not passive store depletion was reported to stimulate the translocation of TRPC3 to the PM in a mechanism that was inhibited by cleavage of VAMP2 (vesicle-associated membrane protein 2) with tetanus toxin (38). Another form of regulation of TRPC3 is by interaction with phospholipase Cγ (22, 39). However, unlike the role of VAMP2, phospholipase Cγ does not affect the acute expression or translocation of TRPC3 but rather the steady-state level of TRPC3 in the PM (22). Stimulation of the epidermal growth factor receptor resulted in translocation of TRPC5 to the PM in a mechanism that was dependent on phosphoinositide 3-kinase, the Rho GTPase Rac1, and phosphatidylinositol-4-phosphate 5-kinase (PIP(5)Kα) (24). Finally, stimulation of the muscarinic M3 receptor resulted in translocation of TRPC6 to the PM in a time course that coincides with activation of Ca^{2+} influx (25).

For the most part, TRPC channel translocation has been studied in cell lines. Whether such a mechanism also operates in native cells is not known. Furthermore, TRPC3, -5, and -6 bind Homers and IP_3Rs (33) (present work). The potential role of Homer and IP_3Rs in this form of regulation of TRP channels activity is not known. Here, we used cells transfected with TRPC3 and Homer 1 (H1) isoforms and cells prepared from WT and $H1^{-/-}$ mice to report that H1 regulates the agonist- and store-dependent translocation and antagonist-mediated retrieval of TRPC3 from the PM. This process requires the dissociation of the IP_3Rs-H1-TRPC3 complex by binding of IP_3 to the IP_3Rs. These findings suggest a novel mechanism by which store depletion leads to activation of TRPC channels and Ca^{2+} influx.

EXPERIMENTAL PROCEDURES

Materials and Solution—Anti-TRPC3 antibodies were a generous gift from Dr. Craig Montell (Johns Hopkins University) or batch 2 from Alomone (Jerusalem, Israel). Anti-IP_3R3 antibodies were from BD Transduction Laboratories, and anti-HA antibodies were from Covance (Princeton, NJ). pRK5-HA-TRPC3, pRK5-HA-Homer 1a, and pRK5-HA-Homer 1c were prepared as detailed elsewhere (33), and pCMV-TRPC3-YFP was generously provided by Dr. Thomas Gudermann (Philipps-Universitat-Marburg, Germany). All biotinylation-related products were purchased from Pierce.

Cell Culture, Transfection, Co-immunoprecipitation, Pull-down Assay, and IP_3 Competition Assay—M3-HEK cells stably expressing the type 3 muscarinic receptor were cultured in Dulbecco's modified Eagle's medium containing 10% fetal bovine serum and 100 units/ml penicillin and streptomycin. Cells were transfected with Lipofectamine Plus reagent (Invitrogen) and used 36–48 h post-transfection. For co-immunoprecipitation (co-IP), the cells were lysed in a buffer containing a protease inhibitor mixture (Roche Applied Sciences). Lysates were incubated overnight at 4 °C with anti-HA antibodies and immunoprecipitated proteins were analyzed by SDS-PAGE. For the IP_3 competition assay, M3-HEK cell lysates and pancreatic microsomal lysates were incubated with or without 100 μM IP_3 for 30 min at 0 °C (ice water bath) to bind IP_3 to the IP_3Rs. GST, GST-H1a, or GST-H1c coupled to beads was then added to the extracts, and the incubation at 0 °C continued for 4–12 h. The beads were washed with lysis buffer, and proteins were released by incubation in SDS sample buffer. Pulled proteins were analyzed by SDS-PAGE and Western blotting. Due to the long incubation required for the pull-down and co-IP assays ($\geq$4.5 h), 100 μM IP_3 was used to ensure the presence of IP_3 during the entire incubation periods.

Isolation of Pancreatic Acinar Cells—The pancreases of 1–2 mice were removed and digested with collagenase and trypsin to isolate single cells to improve access to biotin. Single pancreatic acinar cells were prepared as described before (40). Briefly, the pancreases were finely minced and digested with 4 mg/15 ml collagenase P for 5 min at 37 °C in a solution named PSA that contained 140 mM NaCl, 5 mM KCl, 1 mM $MgCl_2$, 1 mM $CaCl_2$, 10 mM HEPES (pH 7.4 with NaOH), 10 mM glucose, 0.1% bovine serum albumin, and 0.02% soybean trypsin inhibitor. The cells were then washed with Ca^{2+}- and Mg^{2+}-free PBS and treated for 2 min at 37 °C with 0.05% trypsin-EDTA solution (Sigma), washed with PSA, and digested again with collagenase for 3–4 min at 37 °C. Finally, the cells were washed with PSA and stored on ice until use.

Protein Extraction—Mice were scarified, and the tissues of interest were collected. To prepare microsomes, each tissue was washed with a buffer containing 250 mM sucrose, 10 mM HEPES, 1 mM EDTA, 1 mM dithiothreitol, 0.2 mM phenylmethylsulfonyl fluoride and homogenized in 5 ml of buffer by 20 strokes with a Dawn's homogenizer. After centrifugation for 3 min at 1000 rpm, the supernatants were centrifuged for 20 min at 18,000 rpm. The microsomes were dissolved in lysis buffer containing 20 mM Tris, pH 8.0, 137 mM NaCl, 5 mM NaEDTA, 5 mM NaEGTA, 10% glycerol, 0.5% Triton X-100, 0.2 mM phenylmethylsulfonyl fluoride, 50 mM NaF, 20 mM benzamidine and kept on ice for 30 min. Insoluble material was removed by 15-min centrifugation at 14,000 rpm, 4 °C, and the supernatants were collected. Protein concentration in the extracts was measured by the Bradford method.

Surface Biotinylation Assay—Sulfo-NHE-ss-Biotin (Pierce) in PBS supplemented with 1 mM $MgCl_2$ and 0.5 mM $CaCl_2$ was added to control cells or cells treated with agonist, antagonist, or CPA, and the mixtures were incubated for 30 min at 0 °C. Free biotin was quenched by the addition of 1% bovine serum albumin in PBS supplemented with Ca^{2+} and Mg^{2+}, and then the cells were washed once with PBS. Lysates were prepared in lysis buffer by passing 7–10 times through a 27-gauge needle. The lysates were centrifuged at 14,000 rpm for 10 min at 4 °C, and protein concentration in the supernatants was determined. Volume and protein content were adjusted to be the same in all samples, and to each sample was added 10% streptavidin beads (Pierce) in 300 μl. The mixtures were incubated overnight at 4 °C, the beads were washed five times with lysis buffer, and the proteins were extracted by suspending the beads in sample loading buffer. Precipitated proteins were analyzed by Western blot.

Immunocytochemistry—Immunostaining was performed as detailed previously (41). Pancreatic, parotid, or submandibular cells were immobilized on a poly-L-lysine-coated coverslip and were permeabilized with 0.5 ml of cold methanol for 10 min at −20 °C. The samples were washed with PBS, and the nonspecific sites were blocked by a 1-h incubation with a solution containing 5% goat serum, 1% bovine serum albumin, and 0.1% gelatin in PBS (blocking medium). The medium was aspirated and replaced with 50 μl of blocking medium containing control serum or a 1:50 dilution of anti-TRPC3, 1:100 dilution of anti-IP_3R3, and a 1:10 dilution of anti-ZO1 antibodies. After incubation with the primary antibodies overnight at 4 °C and three washes with the incubation buffer, the antibodies were detected with goat anti-rabbit or anti-mouse IgG tagged with fluorescein isothiocyanate or rhodamine. Images were analyzed with a Bio-Rad MRC 1024 confocal microscope.

TRPC3 Current Recording in HEK Cells—M3-HEK cells were transfected with TRPC3 and green fluorescent protein. Whole cell current measurement was accomplished 48 h post-transfection. Cells on coverslips were placed in a perfusion chamber, and green fluorescent protein fluorescence was used to identify the transfected cells. The cells were perfused with bath solution containing 150 mM NaCl, 4 mM KCl, 10 mM HEPES, 0.5 mM EGTA, pH 7.4, with NaOH. Na^+-free bath solution contained 150 mM NMDG-Cl, 10 mM HEPES, 0.5 mM EGTA, pH 7.4 with Tris. The pipette solution contained 140 mM NMDG-Cl, 1 mM $MgCl_2$, 1 mM ATP, 150 mM HEPES, 10 mM EGTA, pH 7.2 with Tris to eliminate the native K^+ current. The patch pipette had a resistance of 2–4 megaohms. After gigaseal (>8 gigaohms) was formed on the cell surface, the whole cell configuration was established by gentle suction. The current was measured by holding the membrane potential at 0 mV and sampled by a 200-ms rapid alterations of membrane potential (RAMPs) between −100 mV and +60 mV. The current at −100 mV was extracted and plotted as a function of time.

Whole Cell Current Recording in Single Pancreatic Acinar Cells—Single pancreatic acinar cells were prepared by a three-step method described previously with some modification (42). The mouse pancreas was minced into fine pieces of ~1 mm^3, washed, and digested with collagenase type IV (40 units/ml for 6 min at 37 °C). The tissue was washed with Ca^{2+}- and Mg^{2+}-free PBS and digested with PBS solution containing 0.025% trypsin for 3 min at 37 °C. The tissue was washed twice with PSA and digested with PSA containing collagenase type IV 20 units/ml for 3 min at 37 °C. Finally, the cells were filtered, suspended in PSA, and kept on ice until use. The cells were perfused with a bath solution containing 140 mM NaC1, 5 mM KCl, 0.5 mM EGTA, 10 mM Hepes (pH 7.4, with NaOH) (divalent free). The patch pipette resistance was 2–5 megaohms when it was filled with internal solution containing 140 mM NMDG-Cl, 1 mM $MgCl_2$, 10 mM EGTA, 5 mM Na_2ATP, and 10 mM HEPES (pH 7.3 with Tris). After a gigaseal (>5 gigaohms) was obtained, the holding potential was changed from 0 to −80 mV. The whole cell configuration was established by a pulse of suction. The current output from the patch clamp amplifier (Axopatch-200B; Axon Instruments) was filtered at 20 Hz, sampled at 1 kHz, and stored in computer with a Digi-Data 1200 interface and pclamp 8.1 software (Axon Instruments).

TIRF Analysis—TRPC3-YFP translocation was monitored in HEK cells expressing TRPC3 alone or co-transfected with H1a. Live cell TIRF imaging was performed with a ×60 objective on a Nikon TIRF microscopy system. Images were analyzed with MetaMorph software (Universal Imaging).

RESULTS AND DISCUSSION

H1a Translocates TRPC3 to the Plasma Membrane—Homer 1a (H1a) has an EVH domain but lacks the multimerizing coiled-coil and leucine zipper domains and dissociates complexes formed by dimerizing H1b/c. H1a is thus a useful tool to study the role of Homer proteins in Ca^{2+} signaling (33). The role of Homer in agonist-mediated translocation of TRPC3 to the plasma membrane (PM) was evaluated by TIRF in HEK293 cells expressing the muscarinic M3 receptors and transfected with TRPC3-YFP or TRPC3-YFP and H1a. The images in Fig. 1*A* and the time lapse movies in the supplement show that a significant portion of TRPC3 was found in intracellular vesicles. Stimulation with carbachol resulted in a rapid disappearance of the vesicles as they fused with the PM. The rapid fusion precluded observing accumulation of the vesicles at the PM, but this was confirmed by surface biotinylation assays in Fig. 1*B*. Removal of carbachol and treatment of the cells with atropine resulted in partial recovery of the vesicles within 40 s of the treatment with atropine. Expression of H1a inhibited translocation of TRPC3-YFP that remained in intracellular vesicles. However, the frequency of finding intracellular vesicles was low, and when found, the vesicles appeared smaller (average size of vesicles in the presence of H1a was 61 ± 4% (n = 32) smaller than in the absence of H1a). These vesicles were not translocated to the PM upon agonist stimulation.

The effect of H1a was quantitated by a biotinylation assay to measure the surface expression of TRPC3. Fig. 1*B* shows that cell stimulation resulted in rapid translocation of TRPC3 to the PM. Expression of H1a increased the level of TRPC3 present at the PM of resting cells to a level caused by cell stimulation. Subsequent stimulation of cells expressing H1a resulted in only a small further increase in PM expression of TRPC3. The dimerizing H1b increased the total cellular level of TRPC3, perhaps by decreasing degradation of the channel, but did not change its surface expression at the resting state or its translocation to the PM by cell stimulation. Similar results were observed with TRPC3-YFP (not shown).

The functional consequences of the effects of H1a and H1b on TRPC3 translocation are depicted in Fig. 1, *C–E*. Fig. 1*C* shows examples of current traces, Fig. 1*D* shows the typical TRPC3 I/V in TRPC3-transfected cells, and Fig. 1*E* is the summary. HEK293 cells transfected with empty vector, H1a alone, or H1b alone did not show a typical TRPC3 current (Fig. 1, *C* and *D*). Resting HEK293 cells expressing TRPC3 showed very small spontaneous TRPC3-specific current. Stimulation of the M3R resulted in activation of TRPC3. In the presence of H1a, mostly spontaneous TRPC3 current was detected, consistent with PM localization of the channel and indicating that TRPC3 was fully active in the presence of H1a. H1b only increased the stimulated activity of TRPC3 (Fig. 1*C*, *red trace*), as expected

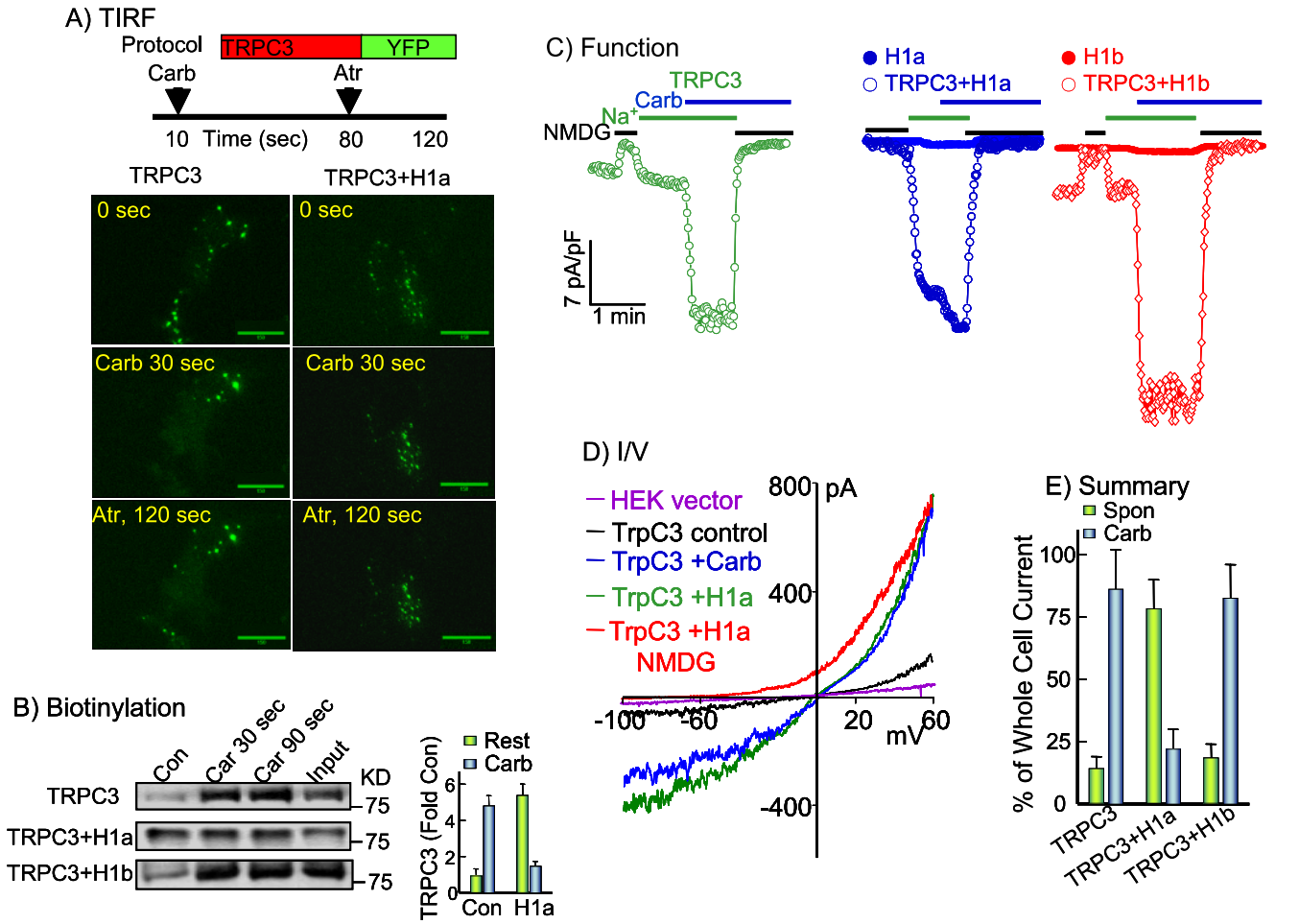

FIGURE 1. **H1a translocates TRPC3 to the plasma membrane.** *A*, HEK293 cells transfected with TRPC3-YFP (*left images*) of TRPC3-YFP and H1a (*right images*) were stimulated with 100 μM carbachol for 60 s and then inhibited with 10 μM atropine for 40 s, and TIRF fluorescence was recorded. *B*, biotinylation assay. HEK293 cells transfected with HA-TRPC3 (*all blots*), H1a (*middle blot*), or H1b (*lower blot*) were stimulated with 100 μM carbachol for the indicated times, and surface TRPC3 was assayed by biotinylation as detailed under "Experimental Procedures." The *columns* are the summary of three experiments showing the -fold increase in TRPC3 at the plasma membrane relative to the level in control, unstimulated cells. The results were corrected for input of TRPC3 and show that most TRPC3 was in the plasma membrane of resting cells expressing TRPC3 and H1a. *C–E*, channel function. The whole cell current was measured at a holding potential of −100 mV in cells transfected with TRPC3 alone (*C*), H1a alone (*solid blue symbols*), TRPC3 and H1a (*open blue symbols*), H1b alone (*solid red symbols*), or TRPC3 and H1b (*open red symbols*), as indicated. Spontaneous current was measured by incubating resting cells with media containing Na^+ of $NMDG^+$, and then the cells were stimulated with 100 μM carbachol to record the stimulated TRPC3 current, as evident from the *I/V* plots in *D*. The summary in *E* is of spontaneous (*Spon*; *green*) or agonist-stimulated current (*Carb*; *blue*) at −100 mV from 4–6 cells, which were normalized for cell capacitance (pA/picofarads) and averaged to obtain the mean ± S.E.

from increased expression of the channel and receptor-mediated translocation to the PM.

IP_3 Dissociates IP_3Rs-H1 Interaction—Co-IP experiments showed that expression of H1b/c increases, whereas expression of H1a decreases, the co-IP of TRPC3 and IP_3 receptors (not shown), suggesting that H1b/c assembles and H1a dissociates TRPC3-H1b/c-IP_3Rs complexes. The question that arises is how disassembly of the complexes occurs under physiological conditions and its role in regulating TRPC3 activity. A clue was provided by a recent crystal structure of the ligand-binding suppressor domain of the IP_3R1, which showed that the Homer binding motif of the IP_3Rs is adjacent to the IP_3 binding core (43). We reasoned that binding of IP_3 to activate the IP_3Rs and evoke Ca^{2+} release from the stores may also allosterically inhibit binding of H1 to the IP_3Rs and dissociate the TRPC3-H1b/c-IP_3Rs complexes. The pull-down (*PD*) assays in Fig. 2*A* indicate that this is the case. GST-H1a and GST-H1c specifically pulled down the native IP_3R3 and transfected TRPC3. Remarkably, the addition of IP_3 inhibited the binding of both H1a and H1c to the IP_3 receptors but did not affect the binding of the Homers to TRPC3.

To determine the functional significance of H1b/c-IP_3R dissociation by IP_3, we measured the effect of IP_3 on modulation of the TRPC3 current by the Homers. Maximal activation of TRPC3 by H1a was verified by showing that infusion of 100 μM IP_3 into cells expressing H1a and TRPC3 did not further activate the channel (Fig. 2*C*). Importantly, infusing the TRPC3 + H1a-expressing cells with recombinant multimerizing H1c recoupled TRPC3 to reduce the spontaneous activity and increase the receptor-activated portion of the current to that found in control cells (Fig. 2*D*). Most notably, IP_3 completely inhibited the effect of H1c (Fig. 2*E*), as expected from inhibition of binding of H1c to the IP_3Rs by IP_3 (Fig. 2*A*). The recoupling indicates that after dissociation of the complex by cell stimulation and binding of IP_3 to the IP_3Rs, the channels remain in

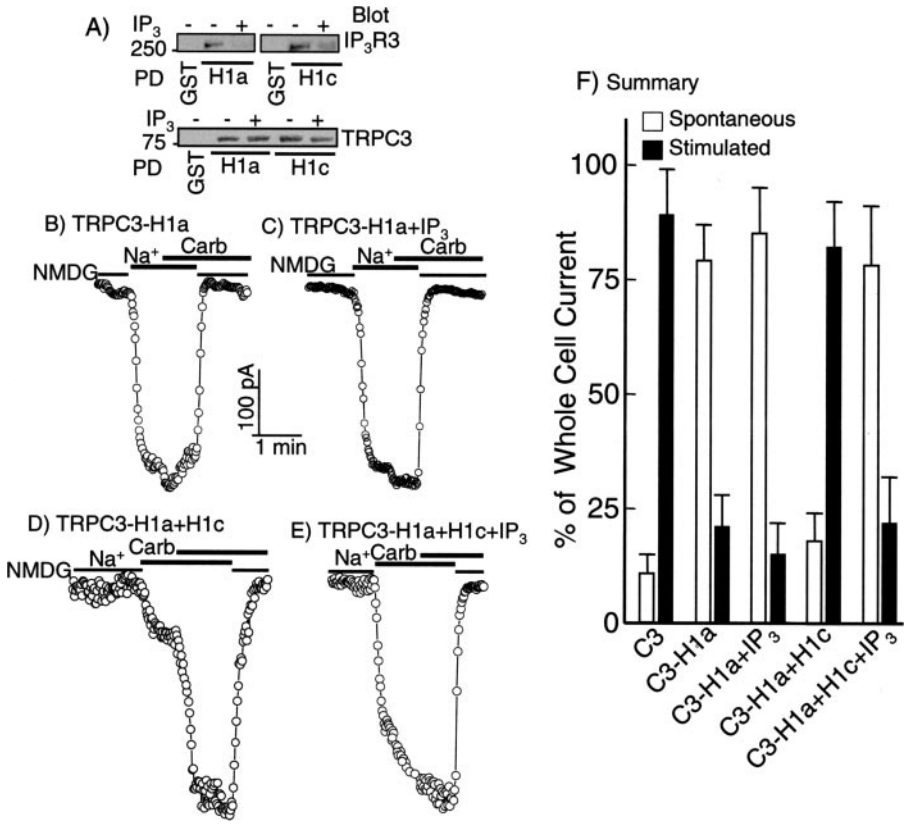

FIGURE 2. **Functional consequences of inhibition by IP_3 of Homers binding to the IP_3R.** *A*, the blots show inhibition by IP_3 of H1a and H1c binding to the IP_3R. Extracts prepared from HEK293 cells transfected with TRPC3 were incubated at 0 °C with and without 100 μM IP_3 and were used to pull down TRPC3-H1b/c-IP_3Rs complexes by beads bound with GST alone (control), GST-H1a, or GST-H1b. Binding of IP_3 to the IP_3Rs inhibited the binding and pulldown (*PD*) of IP_3Rs by H1a and H1b. *B–E*, whole cell current was measured in HEK293 cells transfected with TRPC3 and H1a (*B–E*). The cells were also infused with 100 μM IP_3 to show that, once activated by H1a, the current is no longer sensitive to store depletion (*C*). Cells expressing TRPC3 + H1a were infused with 50 μg of recombinant H1c (*D*) or H1c and 100 μM IP_3 to inhibit binding of H1c to the IP_3Rs. Inward current was measured at a holding potential of −100 mV, and monovalent cation current was evaluated by incubating the cells in medium containing 150 mM $NMDG^+$ or Na^+ and resting or stimulated with 100 μM carbachol. *F*, summary of spontaneous or agonist-stimulated current from 8–13 cells under each condition.

close proximity to allow the recoupling. This point will be further addressed below.

TRPC3 Is Expressed at the Lateral Pole of Polarized Cells—The results in Figs. 1 and 2 suggest that Homers play a role in translocation of TRPC3 to the PM and regulation of its activity. To extend these findings to the *in vivo* situation, we used pancreatic and salivary gland cells, which express high levels of TRPC3. Fig. 3 shows that TRPC3 is expressed mainly at the lateral membrane and next to the apical pole of all cells examined. Previous work used immunohistochemistry to suggest that TRPC3 may be expressed at the luminal membrane of the submandibular gland (44). The more sensitive immunofluorescence localization in Fig. 3*B* shows concentration of TRPC3 and IP_3Rs at the junctional site at the apical pole (*yellow arrowheads*), expression at the lateral and basal poles (*white arrowheads*), and weak expression at the luminal membrane. Transfection in Madin-Darby canine kidney cells grown on permeable support confirmed targeting of TRPC3 mainly to the basolateral membrane, proximal to ZO1 and the same as β-catenin (Fig. 3*C*). The same localization was found with four different anti-TRPC3 antibodies (Montell, Schilling, Alomone, and Sigma).

The specificity of the antibodies used for the staining, the co-IP, and the biotinylation experiments is shown in Fig. 3*D*. The anti-TRPC3 antibodies detected a single band of about 78 kDa in 37 μg of brain and pancreatic extracts. Moreover, the antibodies detected a single band in 6 μg of extract prepared from HEK293 cells transfected with TRPC3-YFP. The anti-IP_3R3 antibodies detected a single band of about 270 kDa in pancreatic and HEK293 cell extracts and two bands in HEK293 cells transfected with green fluorescent protein-IP_3R3 (Fig. 3*D*). Hence, the antibodies used in the present work had the required specificity. The Co-IP experiments in Fig. 3*E* show that in secretory cells and the brain, TRPC3 exists in complexes with IP_3Rs and the plasma membrane Ca^{2+} ATPase pump (PMCA).

Receptor- and Store-dependent Translocation of TRPC3 to the PM—A biotinylation assay was used to follow TRPC3 translocation in native cells. Fig. 4*A* shows that some TRPC3 is present at the PM of resting cells and that stimulation of the G_q-coupled M3 receptors resulted in a robust translocation of TRPC3 to the PM. Significantly, termination of cell stimulation with atropine resulted in retrieval of TRPC3 from the PM. The state of the interaction of IP_3Rs with TRPC3 at the PM was assayed by biotinylation. Fig. 4*B* shows that in unstimulated cells, some IP_3Rs were pulled down by the avidin beads, probably by binding to surface proteins, such as TRPC3. The specificity of the biotinylation is shown by the lack of pulldown of the cytoplasmic protein aldolase. Cell stimulation reduced the amount or the strength of interaction of IP_3Rs with surface proteins. Again, the reduced interaction was reversed by subsequent inhibition of cell stimulation with atropine, indicating that after the dissociation by cell stimulation, the IP_3Rs remain in close proximity to TRPC3 at the PM. That at least one of the PM proteins interacting with IP_3Rs is TRPC3 is shown in Fig. 4*C*, which shows that IP of TRPC3 co-immunoprecipitated IP_3R3, the co-IP was reduced by cell stimulation, and the IP_3Rs-TRPC3 complex was reformed by inhibition of carbachol-stimulated cells with atropine.

Although several studies (17, 19, 28, 45, 46), including ours (18, 30), suggested that TRPC3 can function as SOCs, others concluded that this is not the case (15, 47, 48). However, the behavior of TRPC3 in native cells was examined before only in one study using pontine neurons from P3–P8 rats. In these cells, activation of TRPC3 required IP_3-mediated Ca^{2+} release,

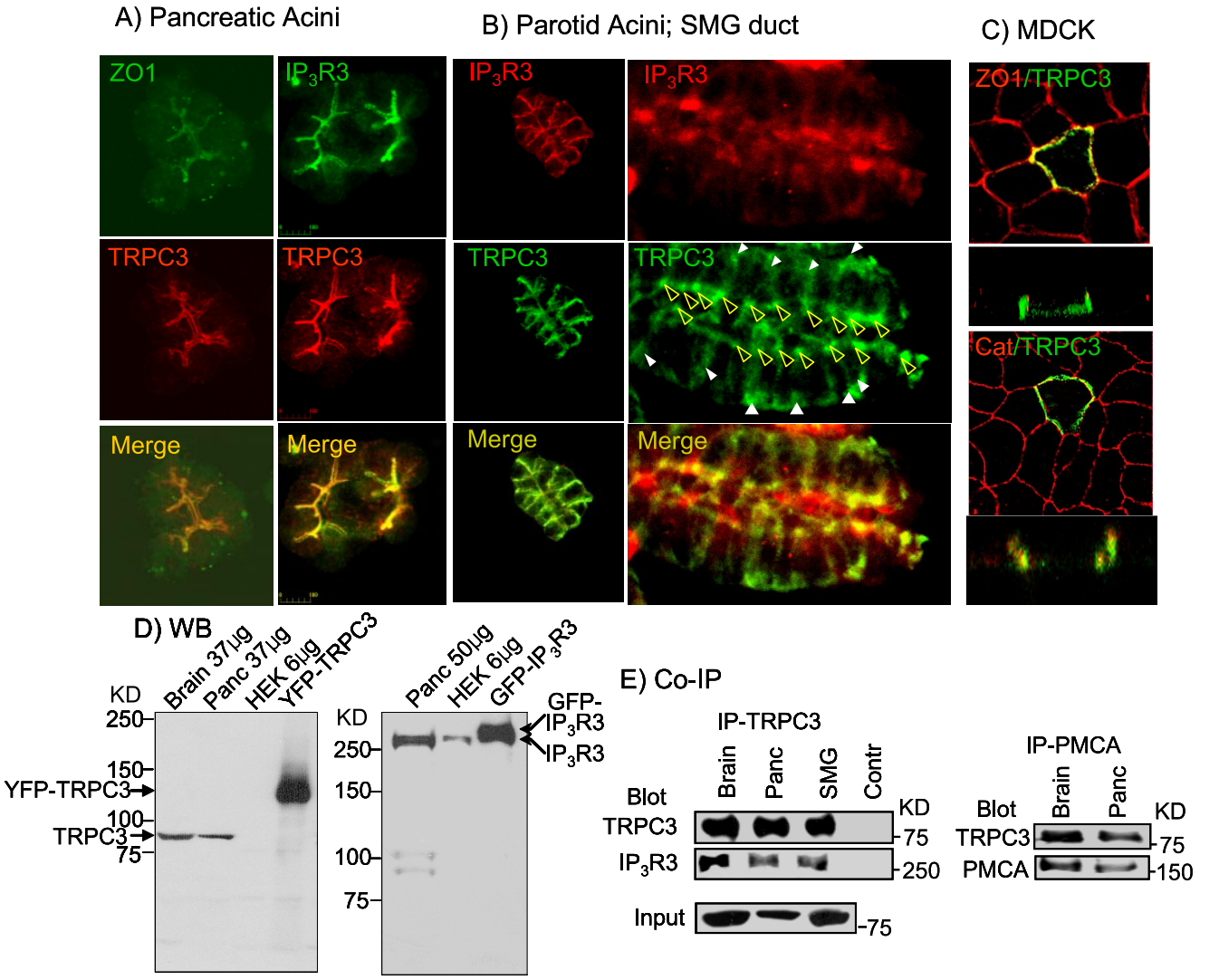

FIGURE 3. **Basolateral localization of TRPC3.** Large clusters of pancreatic (*A*) and parotid (*B*, *left*) acini or submandibular duct (*B*, *right*) were co-stained for TRPC3 (*green*) and ZO1 (*A*) or IP_3Rs (*A* and *B*, *red*). The *yellow arrowheads* in the duct mark expression of TRPC3 at the apical pole junctions, and the *white arrowheads* mark the basolateral membrane. In *C*, HA-TRPC3 was expressed in polarized Madin-Darby canine kidney cells, and the cells were co-stained for TRPC3 (*green*) and ZO1 (*upper images*) or β-catenin (*lower images*) (*red*). In each *panel*, the *upper image* is the *x*/*y* scan at the apical region, and the *lower image* is the *z* scan. *D* shows the high specificity of the antibodies used in the present work as revealed by blotting for TRPC3 (*left*) and IP_3R3 (*right*) of extracts prepared from the mouse brain and pancreas (*panc*) from untransfected HEK293 cells of HEK293 cells transfected with TRPC3-YFP or green fluorescent protein (*GFP*)-IP_3R3, as indicated. In *E*, native TRPC3 (*left*) or plasma membrane Ca^{2+} ATPase pump (PMCA) (*right*) was immunoprecipitated, and the precipitates were probed for TRPC3 and IP_3Rs (*left*) or TRPC3 and PMCA (*right*).

although the channel could not be activated by treating the cells with thapsigargin (49). Here we examined the role of Ca^{2+} stores in the translocation of TRPC3. Fig. 4, *A* and *B*, shows that store depletion with the SERCA pump inhibitor CPA was as effective as agonist stimulation in causing TRPC3 translocation to the PM and in altering its interaction with IP_3Rs.

TRPC3 translocation was dependent on both IP_3Rs and depletion of stored Ca^{2+}. Store depletion with CPA reduced the co-IP of IP_3Rs and TRPC3 in native cells (Fig. 4*C*). Furthermore, Fig. 4*D* shows that inhibition of the IP_3Rs with xestospongin C (*Xest C*) inhibited the agonist- and CPA-mediated translocation of TRPC3 to the PM. Since inhibition of SERCA pumps with CPA depletes the Ca^{2+} stores also in the presence of Xest C, inhibition of TRPC3 translocation by CPA indicates that the translocation required functional IP_3Rs. The protocol of Fig. 4*E* was designed to show that TRPC3 translocation and retrieval were dependent on Ca^{2+} content of the stores. Acinar cells were incubated in Ca^{2+}-free medium and stimulated with carbachol to deplete stored Ca^{2+}, which resulted in the usual translocation of TRPC3 to the PM. Inhibition by atropine while the cells were kept in Ca^{2+}-free medium to prevent store reloading inhibited retrieval of TRPC3. The subsequent addition of Ca^{2+} to the medium to reload the stores resulted in retrieval of TRPC3 from the PM. We have previously used the same protocol to show that SOCs remained fully active as long as the stores were not allowed to reload with Ca^{2+} and were inhibited only when the stores were reloaded with Ca^{2+} (50, 51).

The implication of the results in Figs. 3 is that translocation of TRPC3 to the PM is dependent on IP_3Rs and on store Ca^{2+} content. This indicates that (*a*) *in vivo* TRPC3 behaves as SOCs, (*b*) TRPC3 is a subunit of SOCs, and (*c*) *in vivo* the TRPC3-

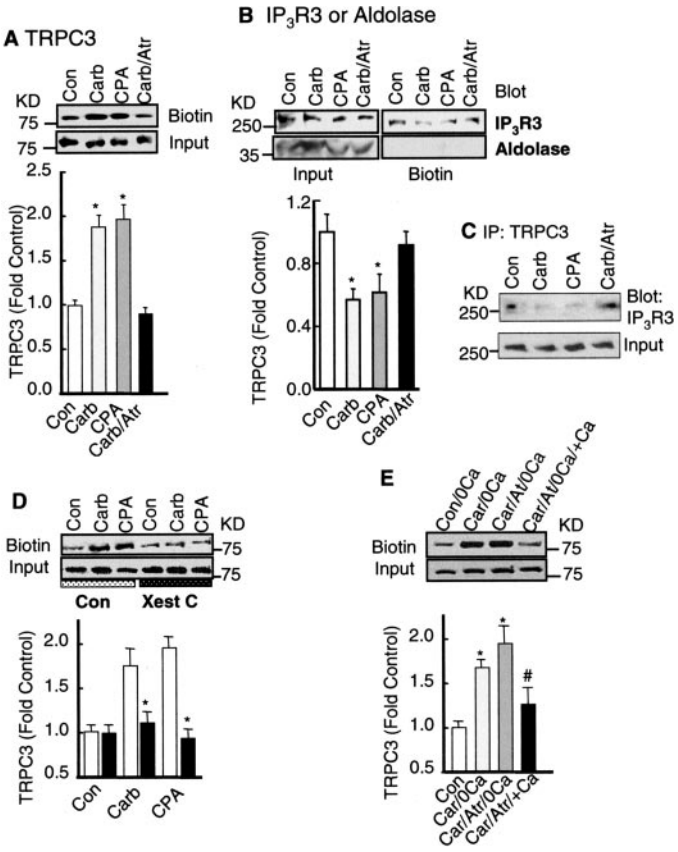

FIGURE 4. **IP_3Rs- and store-dependent translocation and retrieval of TRPC3 from the plasma membrane.** *A*, pancreatic acinar cells from WT mice were stimulated with 1 mM carbachol or treated with 30 μM CPA for 5 min or stimulated with carbachol for 2 min and inhibited with 10 μM atropine for 3 min. The cell surface proteins were biotinylated, and extracts were prepared to pull down and analyze plasma membrane levels of TRPC3. The *columns* show a summary of 4–5 experiments. *, $p < 0.01$ relative to unstimulated WT cells. *B*, the same protocol as in *A* was used, except that the blots were analyzed for IP_3R3. For a control, the blots were analyzed for the cytosolic protein aldolase. *C*, extracts were prepared from acini treated as in *A* and were used to immunoprecipitate TRPC3 and blot for IP_3R3 to assay for co-IP of IP_3Rs and TRPC3. *D*, the same protocol as in *A* was used, except that a portion of the cells was treated with 5 μM xestospongin C (*Xest C*) for 10 min before treatment with carbachol or CPA. The *columns* summarize the results of three similar experiments. *E*, effect of store Ca^{2+} content on TRPC3 retrieval. Cells in Ca^{2+}-free medium were stimulated with carbachol for 5 min (*Car/0Ca*) or with carbachol for 2 min and inhibited with atropine for 3 min (*Car/Atr/0Ca*). Ca^{2+} to a final concentration of 2 mM was added to cells treated with carbachol and atropine in Ca^{2+}-free medium, and the incubation continued for an additional 3 min (*Car/Atr/0Ca/+Ca*). The cells were then used to determine surface expression of TRPC3. The columns show the summary of three similar experiments. *, $p < 0.01$ relative to unstimulated cells; #, $p < 0.05$ relative to *Car/Atr/0Ca* cells. *Con*, control.

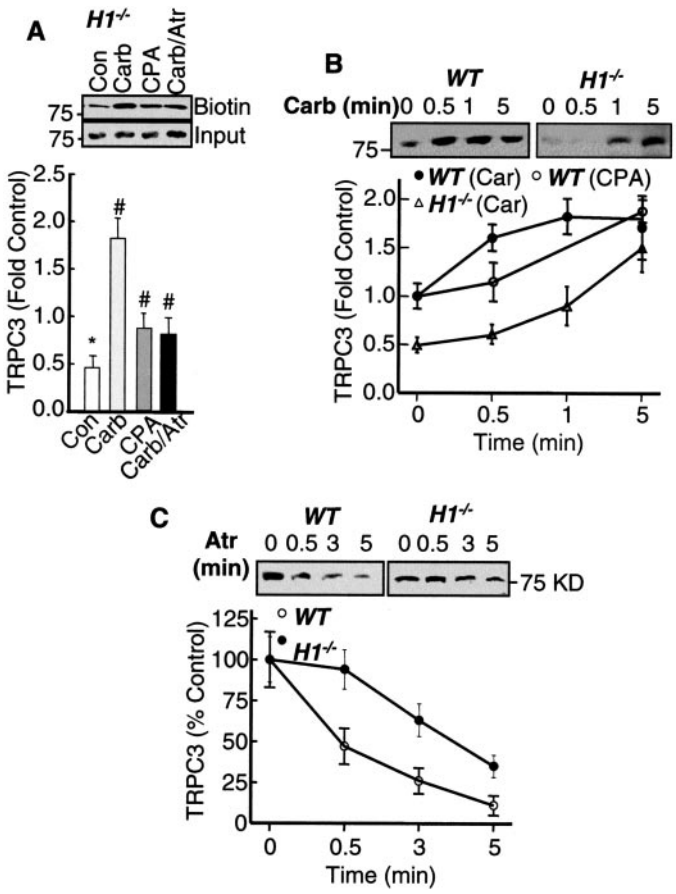

FIGURE 5. **H1 facilitates IP_3Rs- and store-dependent translocation and retrieval of TRPC3 from the plasma membrane.** *A*, pancreatic acinar cells from $H1^{-/-}$ mice were treated as in Fig. 4*A*, and plasma membrane levels of TRPC3 were analyzed by biotinylation. The *columns* show the summary of 4–5 experiments. *, $p < 0.01$ relative to unstimulated WT cells; #, $p < 0.05$ from unstimulated $H1^{-/-}$ cells. *B*, effect of H1 on time course of TRPC3 translocation. WT (●) and $H1^{-/-}$ acinar cells (△) were stimulated with 1 mM carbachol (● and △) or treated with 30 μM CPA (○) for the indicated times, and surface TRPC3 was determined by biotinylation. *B* shows a typical blot and the summary of 4–5 similar experiments. *C*, effect of H1 on time course of TRPC3 retrieval. WT (○) and $H1^{-/-}$ acinar cells (●) were stimulated with 1 mM carbachol for 5 min, and samples were removed to determine surface level of TRPC3 before termination of cell stimulation with 10 μM atropine. Samples were removed at the indicated times to measure the rate of TRPC3 retrieval. *Con*, control.

associated SOCs are regulated in part by translocation to the PM.

Homer 1 Regulates the Rate of TRPC3 Translocation and Retrieval—The role of Homers in agonist- and store-dependent TRPC3 translocation to the PM was examined using pancreatic acinar cells from WT and $H1^{-/-}$, $H2^{-/-}$, and $H3^{-/-}$ mice. Deletion of Homer 2 and Homer 3 had no apparent effect on TRPC3 translocation (not shown), indicating that the effects described below are specific to Homer 1 (H1). Deletion of H1 had no effect on overall expression of TRPC3 but reduced the steady-state level of TRPC3 at the PM by about 50% (Fig. 5*A*). This is probably an adaptation to reduce the spontaneous activity of TRPC3 at the PM (see Ref. 33) (see below). Stimulation of $H1^{-/-}$ cells resulted in translocation of TRPC3 to increase its level at the PM to that found in stimulated WT cells. However, store depletion by CPA was less effective in stimulating TRPC3 translocation in $H1^{-/-}$ cells. Furthermore, inhibition of cell stimulation by atropine for 3 min resulted in only partial retrieval of TRPC3 from the PM.

To determine the reason for the poor TRPC3 translocation stimulated by store depletion and its poor retrieval on termination of cell stimulation in $H1^{-/-}$ cells, we compared the time course of the translocation and retrieval of TRPC3 in WT and $H1^{-/-}$ cells. Fig. 5*B* shows that most TRPC3 translocation was completed within 30 s of stimulation with agonist, whereas little translocation was measured after 30 s of treatment with CPA. Comparable translocation was measured after 5 min of treatment with agonist or CPA, consistent with the fast and slow depletion of the Ca^{2+} stores by agonist stimulation and inhibition of SERCA pump, respectively. Fig. 4*B* shows that deletion

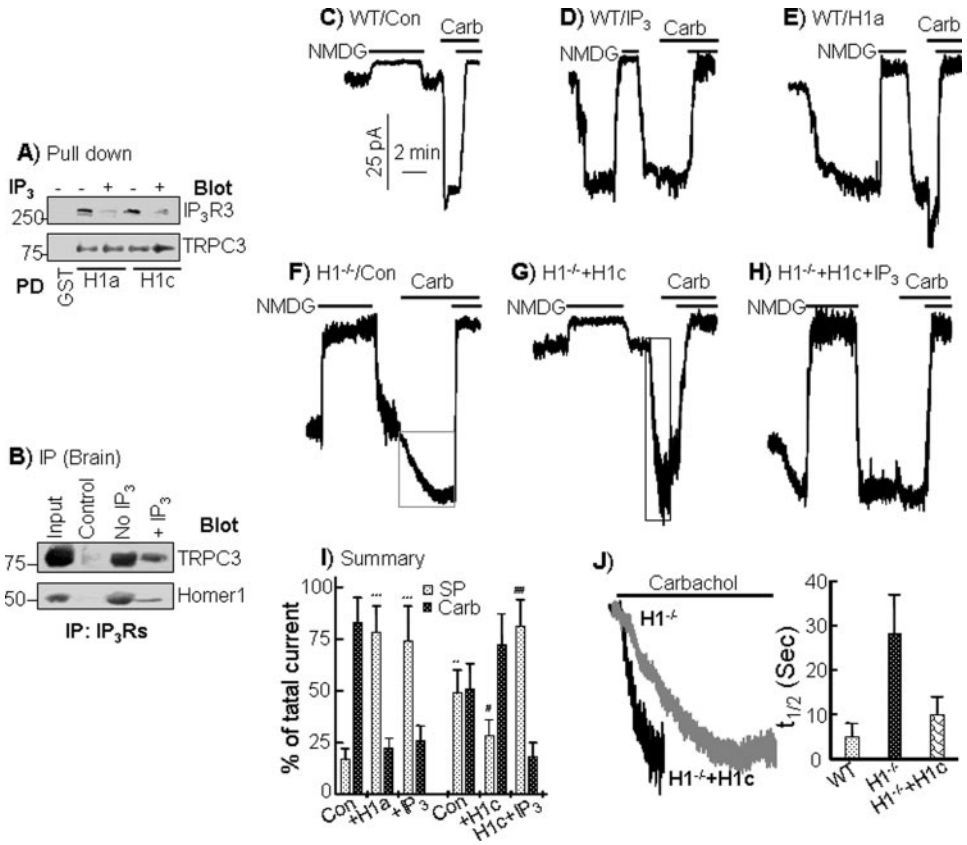

FIGURE 6. **Functional consequences of inhibition by IP_3 of Homers binding to the IP_3 in native cells.** *A*, inhibition by IP_3 of H1a and H1c binding to the IP_3Rs. Extracts prepared from the pancreas were incubated at 0 °C with and without 10 μM IP_3 and used to form and pull down TRPC3-H1b/c-IP_3Rs complexes by beads coupled to GST alone (control), GST-H1a, or GST-H1b. Binding of IP_3 to the IP_3Rs inhibited the binding and pulldown (*PD*) of IP_3 receptors, but not of TRPC3, by H1a and H1b. *B*, effect of IP_3 on co-IP of IP_3Rs-H1. IP_3Rs were immunoprecipitated from brain extracts incubated in the presence or absence of IP_3, and the precipitates were probed for co-IP of TRPC3 and H1. In the control, anti-IP_3Rs antibodies were not added. *C–H*, WT (*C–E*) and $H1^{-/-}$ (*F–H*) pancreatic acinar cells were used to measure the monovalent cation current at −60 mV using a pipette solution containing 10 mM EGTA and bath solutions containing 150 mM Na^+ or $NMDG^+$. Where indicated by the *bars*, the cells were stimulated with 1 mM carbachol (*Carb*). *C*, the WT control (*Con*). The pipette solution contained 10 μM IP_3 in *D* and 50 μg of H1a in *E* to show that agonist stimulation, store depletion with IP_3, and H1a activate the same current. *F*, the control for $H1^{-/-}$ cells, showing the increased spontaneous current and the slow agonist-dependent activation of the residual current. In *G*, the cells were infused with H1c, which reduced the spontaneous current and increased the size and the rate of current activation by agonist stimulation. The portion of the current activated by agonist in *F* (*black trace*) and *G* (*gray trace*) was rescaled and is replotted in *J*, which also shows the summary of $t_{1/2}$ for current activation in WT, $H1^{-/-}$ cells, and $H1^{-/-}$ cells infused with H1c in 6–9 experiments. In *H*, the cells were infused with H1c and 10 μM IP_3, which inhibited the effect of H1c. *I* summarizes the spontaneous (*dotted columns*) and agonist-activated current (*filled columns*) under each condition. ***, $p < 0.01$ from WT control; **, $p < 0.05$ relative to WT control; #, $p < 0.05$ from control $H1^{-/-}$ cells; ##, $p < 0.01$ from +H1c in $H1^{-/-}$ cells.

down (not shown) and co-IP from brain extract (Fig. 6*B*). Brain extract was used for the co-IP experiments, since the level of H1 in the pancreas was low and could not be reliably detected in the immunoprecipitate. Fig. 6*B* shows that IP of IP_3Rs co-immunoprecipitated TRPC3 and H1, and binding of IP_3 to the IP_3Rs reduced the co-IP of TRPC3 and H1 with the IP_3Rs.

TRPC3 functions as a nonselective monovalent cation channel (18, 52). Therefore, we measured the properties of the monovalent cation current in WT and $H1^{-/-}$ acinar cells. The cells were dialyzed with 10 mM EGTA to inhibit all Ca^{2+}-activated currents, prevent inhibition of TRPC3 current by $[Ca^{2+}]_i$, and facilitate store depletion. Fig. 5*C* shows that resting WT cells have a small spontaneous cation current, and cell stimulation prominently and rapidly activated the current. Interestingly, infusion of IP_3 (Fig. 6*D*) or recombinant H1a (Fig. 6*E*) maximally activated the same cation current, as evident from the minimal effect of agonist stimulation after activation of the current by IP_3 or H1a.

Parallel measurement in $H1^{-/-}$ cells showed that about half of the cation current was spontaneously active in these cells. Stimulation of $H1^{-/-}$ cells resulted in further activation of the current. However, the current was only slowly activated, consistent with the slow translocation of TRPC3 to the PM shown in Fig. 5*B*. The most significant findings for the purpose of the present discussion are shown in Fig. 6, *G* and *H*, and are summaries in Fig. 6, *I* and *J*. Fig. 6*G* shows that infusion of recombinant dimerizing H1c recoupled the current to reduce the spontaneous and increase the receptor-stimulated current. In addition, H1c increased the rate of current activation by agonist (Fig. 6*J*), as expected from the effect of H1 on the rate of TRPC3 translocation. Fig. 6*H* shows that IP_3 completely inhibited the effect of H1c, as predicted from inhibition of binding of H1c to the IP_3Rs by IP_3 shown in Fig. 6*A*.

Pancreatic acinar cells express TRPC3, TRPC6, and probably other TRP channels. Preliminary studies showed that TRPC3 and TRPC6 exist in Ca^{2+} signaling complexes with other Ca^{2+}-signaling proteins, including IP_3Rs and Homers (not shown). The excellent agreement between regulation of recombinant TRPC3 by Homers and IP_3Rs in HEK293 cells of H1 markedly reduced the rate of TRPC3 translocation in response to agonist stimulation. Furthermore, Fig. 5*C* shows that deletion of H1 also reduced the rate of TRPC3 retrieval initiated by atropine inhibition of stimulated cells. Thus, the combined results in Fig. 5 show that H1 regulates the rate of stores and IP_3Rs-mediated translocation and retrieval of TRPC3.

Functional Correlate—To determine the relationship between IP_3Rs, H1 and TRPC3 in native cells, we measured the effect of IP_3 on the interaction between the proteins. As was found in HEK293 cells (Fig. 2*A*), GST-H1a and GST-H1c specifically pulled down TRPC3 and IP_3R3 from pancreatic acinar cell extracts, and binding of IP_3 to the IP_3Rs dissociated the Homers-IP_3Rs interaction without dissociating the Homers from TRPC3 (Fig. 6*A*). Similar results were also obtained by pull-

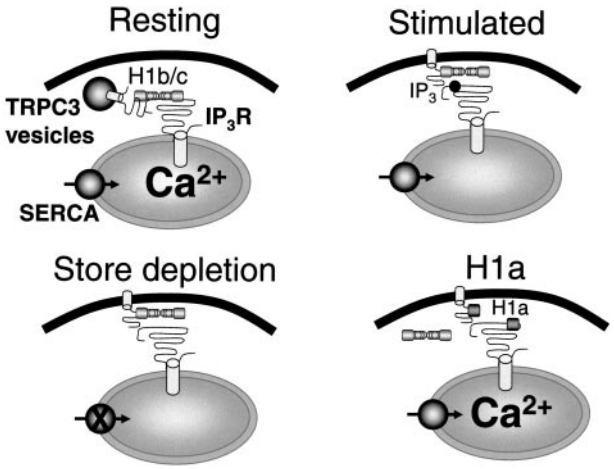

FIGURE 7. **A model depicting the role of H1 in controlling TRPC channels translocation and retrieval.** In resting cells, TRPC3 is in TRPC3-H1b/c-IP_3Rs complexes and is inactive. Cell stimulation generates IP_3 to release Ca^{2+} from internal stores and dissociate the interaction between H1 and IP_3Rs but not between TRPC3 and IP_3Rs to generate IP_3-TRPC3-H1 complexes that fuse with the plasma membrane to activate Ca^{2+} influx. The same translocatable and active complexes can also be formed by store depletion or by H1a that lacks the multimerizing coiled-coil domain of H1b/c.

and native TRPC3 in pancreatic and salivary gland cells, including properties of the nonselective monovalent cation current, suggest that TRPC3 is a major component of SOCs in native cells and that other TRP channels that participate in SOCs are likely to be regulated by H1. Previous work with TRPC3 and TRPC6 expressed individually in HEK293 cells concluded that both channels do not behave as SOCs (15). Furthermore, TRPC3 and TRPC6 did not translocate to the PM in response to store depletion (25, 38). The present findings emphasize the need to study the TRPC channels *in vivo* to understand their physiological behavior and contribution to Ca^{2+} influx. *In vivo* TRPC3 behaves as SOCs and appears to contribute to agonist-stimulated and store-dependent Ca^{2+} influx.

The key findings of the present work are that binding of IP_3 to the IP_3Rs inhibited binding of H1 to the IP_3Rs to disassemble the TRPC3-H1b/c-IP_3Rs complexes and that H1 regulates the rates of translocation and retrieval of TRPC3 from the PM. At the same time, in a previous work we showed that IP_3R (18) and its N-terminal domain (30) bound with IP_3 activate TRPC3. TRPC3- and IP_3R-interacting domains were subsequently identified (28), and the IP_3R domain that binds to TRPC3 was sufficient to activate TRPC3 (32). Since cell stimulation and binding of IP_3 to IP_3Rs result in dissociation of H1 from IP_3Rs and reduced interaction of IP_3Rs with TRPC3, we propose that H1 may have two roles in controlling TRPC3 activity: facilitation of TRPC3 translocation and retrieval from the PM and strengthening of the interaction and gating of TRPC3 by IP_3Rs. The model in Fig. 7 attempts to account for both effects of H1. In resting cells, TRPC3 exists in a complex with H1 and IP_3 receptors. IP_3Rs and TRPC3 also interact directly, and this interaction is stabilized by H1. While in the complex, TRPC3 is not active, whether the TRPC3-H1b/c-IP_3Rs complex is at the PM or in intracellular vesicles. IP_3 generated by receptor stimulation binds to the IP_3Rs to release Ca^{2+} from the stores and dissociate between IP_3Rs and H1 to form the IP_3Rs-TRPC3-H1b/c complex, in which interaction between IP_3Rs-TRPC3 is flexible and is not maintained in extracts of stimulated cells or extracts incubated with IP_3. The IP_3Rs-TRPC3-H1 complex rapidly translocates to the PM. The IP_3Rs-TRPC3-H1b/c complex is active and mediates Ca^{2+} influx. Maintained binding of IP_3 to the IP_3Rs and interaction of IP_3Rs with TRPC3 is required for activation of TRPC3 (18, 28, 30, 32). H1a can also dissociate the IP_3Rs-H1-TRPC3 complexes to form IP_3Rs-TRPC3-H1a complexes that translocate and fuse with the PM. As long as the IP_3Rs is bound with IP_3, it does not bind to H1, and TRPC3 remains active at the PM. Termination of cell stimulation results in hydrolysis of IP_3, reloading of the stores with Ca^{2+}, restoration of binding of H1 to IP_3Rs, and stabilization of the TRPC3-H1b/c-IP_3Rs complexes and retrieval of TRPC3 from the PM.

Recent studies identified STIM1 (stromal interaction molecule-1) as a sensor of ER Ca^{2+} stores that is essential for agonist- and store-dependent activation of I_{crac} (53) and SOCs (54, 55). Cell stimulation translocates STIM1 from the ER to the PM (53). Hence, regulation of SOCs by STIM1 and H1 are probably two different modes of channel regulation.

REFERENCES

1. Parekh, A. B., and Putney, J. W., Jr. (2005) *Physiol. Rev.* **85,** 757–810
2. Feske, S., Gwack, Y., Prakriya, M., Srikanth, S., Puppel, S. H., Tanasa, B., Hogan, P. G., Lewis, R. S., Daly, M., and Rao, A. (2006) *Nature* **441,** 179–185
3. Peinelt, C., Vig, M., Koomoa, D. L., Beck, A., Nadler, M. J., Koblan-Huberson, M., Lis, A., Fleig, A., Penner, R., and Kinet, J. P. (2006) *Nat. Cell Biol.* **8,** 771–773
4. Zhang, S. L., Yeromin, A. V., Zhang, X. H., Yu, Y., Safrina, O., Penna, A., Roos, J., Stauderman, K. A., and Cahalan, M. D. (2006) *Proc. Natl. Acad. Sci. U. S. A.* **103,** 9357–9362
5. Soboloff, J., Spassova, M. A., Tang, X. D., Hewavitharana, T., Xu, W., and Gill, D. L. (2006) *J. Biol. Chem.* **281,** 20661–20665
6. Nilius, B., and Droogmans, G. (2001) *Physiol. Rev.* **81,** 1415–1459
7. Tiruppathi, C., Freichel, M., Vogel, S. M., Paria, B. C., Mehta, D., Flockerzi, V., and Malik, A. B. (2002) *Circ. Res.* **91,** 70–76
8. Wu, X., Babnigg, G., and Villereal, M. L. (2000) *Am. J. Physiol.* **278,** C526–C536
9. Wu, X., Babnigg, G., Zagranichnaya, T., and Villereal, M. L. (2002) *J. Biol. Chem.* **277,** 13597–13608
10. Wu, X., Zagranichnaya, T. K., Gurda, G. T., Eves, E. M., and Villereal, M. L. (2004) *J. Biol. Chem.* **279,** 43392–43402
11. Liu, X., Singh, B. B., and Ambudkar, I. S. (2003) *J. Biol. Chem.* **278,** 11337–11343
12. Obukhov, A. G., and Nowycky, M. C. (2004) *J. Cell. Physiol.* **201,** 227–235
13. Strubing, C., Krapivinsky, G., Krapivinsky, L., and Clapham, D. E. (2001) *Neuron* **29,** 645–655
14. Yildirim, E., Kawasaki, B. T., and Birnbaumer, L. (2005) *Proc. Natl. Acad. Sci. U. S. A.* **102,** 3307–3311
15. Hofmann, T., Obukhov, A. G., Schaefer, M., Harteneck, C., Gudermann, T., and Schultz, G. (1999) *Nature* **397,** 259–263
16. Gudermann, T., Hofmann, T., Mederos y Schnitzler, M., and Dietrich, A. (2004) *Novartis Found. Symp.* **258,** 103–118
17. Trebak, M., Bird, G. S., McKay, R. R., and Putney, J. W., Jr. (2002) *J. Biol. Chem.* **277,** 21617–21623
18. Kiselyov, K., Xu, X., Mozhayeva, G., Kuo, T., Pessah, I., Mignery, G., Zhu, X., Birnbaumer, L., and Muallem, S. (1998) *Nature* **396,** 478–482
19. Vazquez, G., Lievremont, J. P., St, J. B. G., and Putney, J. W., Jr. (2001) *Proc. Natl. Acad. Sci. U. S. A.* **98,** 11777–11782
20. Berridge, M. J. (1995) *Biochem. J.* **312,** 1–11
21. Patterson, R. L., van Rossum, D. B., and Gill, D. L. (1999) *Cell* **98,** 487–499
22. van Rossum, D. B., Patterson, R. L., Sharma, S., Barrow, R. K., Kornberg,

M., Gill, D. L., and Snyder, S. H. (2005) *Nature* **434,** 99–104
23. Yao, Y., Ferrer-Montiel, A. V., Montal, M., and Tsien, R. Y. (1999) *Cell* **98,** 475–485
24. Bezzerides, V. J., Ramsey, I. S., Kotecha, S., Greka, A., and Clapham, D. E. (2004) *Nat. Cell Biol.* **6,** 709–720
25. Cayouette, S., Lussier, M. P., Mathieu, E. L., Bousquet, S. M., and Boulay, G. (2004) *J. Biol. Chem.* **279,** 7241–7246
26. Smani, T., Zakharov, S. I., Csutora, P., Leno, E., Trepakova, E. S., and Bolotina, V. M. (2004) *Nat. Cell Biol.* **6,** 113–120
27. Randriamampita, C., and Tsien, R. Y. (1993) *Nature* **364,** 809–814
28. Boulay, G., Brown, D. M., Qin, N., Jiang, M., Dietrich, A., Zhu, M. X., Chen, Z., Birnbaumer, M., Mikoshiba, K., and Birnbaumer, L. (1999) *Proc. Natl. Acad. Sci. U. S. A.* **96,** 14955–14960
29. Delmas, P., Wanaverbecq, N., Abogadie, F. C., Mistry, M., and Brown, D. A. (2002) *Neuron* **34,** 209–220
30. Kiselyov, K., Mignery, G. A., Zhu, M. X., and Muallem, S. (1999) *Mol. Cell* **4,** 423–429
31. Tang, J., Lin, Y., Zhang, Z., Tikunova, S., Birnbaumer, L., and Zhu, M. X. (2001) *J. Biol. Chem.* **276,** 21303–21310
32. Zhang, Z., Tang, J., Tikunova, S., Johnson, J. D., Chen, Z., Qin, N., Dietrich, A., Stefani, E., Birnbaumer, L., and Zhu, M. X. (2001) *Proc. Natl. Acad. Sci. U. S. A.* **98,** 3168–3173
33. Yuan, J. P., Kiselyov, K., Shin, D. M., Chen, J., Shcheynikov, N., Kang, S. H., Dehoff, M. H., Schwarz, M. K., Seeburg, P. H., Muallem, S., and Worley, P. F. (2003) *Cell* **114,** 777–789
34. Fagni, L., Worley, P. F., and Ango, F. (2002) *Sci. STKE 2002*, RE8
35. Roderick, H. L., and Bootman, M. D. (2003) *Curr. Biol.* **13,** R976–R978
36. Tu, J. C., Xiao, B., Yuan, J. P., Lanahan, A. A., Leoffert, K., Li, M., Linden, D. J., and Worley, P. F. (1998) *Neuron* **21,** 717–726
37. Xiao, B., Tu, J. C., Petralia, R. S., Yuan, J. P., Doan, A., Breder, C. D., Ruggiero, A., Lanahan, A. A., Wenthold, R. J., and Worley, P. F. (1998) *Neuron* **21,** 707–716
38. Singh, B. B., Lockwich, T. P., Bandyopadhyay, B. C., Liu, X., Bollimuntha, S., Brazer, S. C., Combs, C., Das, S., Leenders, A. G., Sheng, Z. H., Knepper, M. A., Ambudkar, S. V., and Ambudkar, I. S. (2004) *Mol. Cell* **15,** 635–646
39. Patterson, R. L., van Rossum, D. B., Ford, D. L., Hurt, K. J., Bae, S. S., Suh, P. G., Kurosaki, T., Snyder, S. H., and Gill, D. L. (2002) *Cell* **111,** 529–541
40. Zeng, W., Xu, X., Popov, S., Mukhopadhyay, S., Chidiac, P., Swistok, J., Danho, W., Yagaloff, K. A., Fisher, S. L., Ross, E. M., Muallem, S., and Wilkie, T. M. (1998) *J. Biol. Chem.* **273,** 34687–34690
41. Lee, M. G., Xu, X., Zeng, W., Diaz, J., Wojcikiewicz, R. J., Kuo, T. H., Wuytack, F., Racymaekers, L., and Muallem, S. (1997) *J. Biol. Chem.* **272,** 15765–15770
42. Zeng, W., Mak, D. O., Li, Q., Shin, D. M., Foskett, J. K., and Muallem, S. (2003) *Curr. Biol.* **13,** 872–876
43. Bosanac, I., Yamazaki, H., Matsu-Ura, T., Michikawa, T., Mikoshiba, K., and Ikura, M. (2005) *Mol. Cell* **17,** 193–203
44. Bandyopadhyay, B. C., Swaim, W. D., Liu, X., Redman, R., Patterson, R. L., and Ambudkar, I. S. (2005) *J. Biol. Chem.* **280,** 12908–12916
45. Birnbaumer, L., Boulay, G., Brown, D., Jiang, M., Dietrich, A., Mikoshiba, K., Zhu, X., and Qin, N. (2000) *Recent Prog. Horm. Res.* **55,** 127–161
46. Liu, X., Bandyopadhyay, B. C., Singh, B. B., Groschner, K., and Ambudkar, I. S. (2005) *J. Biol. Chem.* **280,** 21600–21606
47. Trebak, M., Bird, G. S. J., McKay, R. R., Birnbaumer, L., and Putney, J. W., Jr. (2003) *J. Biol. Chem.* **278,** 16244–16252
48. Venkatachalam, K., Ma, H. T., Ford, D. L., and Gill, D. L. (2001) *J. Biol. Chem.* **276,** 33980–33985
49. Li, H. S., Xu, X. Z., and Montell, C. (1999) *Neuron* **24,** 261–273
50. Muallem, S., Fimmel, C. J., Pandol, S. J., and Sachs, G. (1986) *J. Biol. Chem.* **261,** 2660–2667
51. Pandol, S. J., Schoeffield, M. S., Fimmel, C. J., and Muallem, S. (1987) *J. Biol. Chem.* **262,** 16963–16968
52. Hurst, R. S., Zhu, X., Boulay, G., Birnbaumer, L., and Stefani, E. (1998) *FEBS Lett.* **422,** 333–338
53. Roos, J., DiGregorio, P. J., Yeromin, A. V., Ohlsen, K., Lioudyno, M., Zhang, S., Safrina, O., Kozak, J. A., Wagner, S. L., Cahalan, M. D., Velicelebi, G., and Stauderman, K. A. (2005) *J. Cell Biol.* **169,** 435–445
54. Liou, J., Kim, M. L., Do Heo, W., Jones, J. T., Myers, J. W., Ferrell, J. E., Jr., and Meyer, T. (2005) *Curr. Biol.* **15,** 1235–1241
55. Zhang, S. L., Yu, Y., Roos, J., Kozak, J. A., Deerinck, T. J., Ellisman, M. H., Stauderman, K. A., and Cahalan, M. D. (2005) *Nature* **437,** 902–905